

# Statistical Design of Nonrecursive Digital Filters

DAVID C. FARDEN, STUDENT MEMBER, IEEE, AND LOUIS L. SCHARF, MEMBER, IEEE

*Abstract*—The problem of designing a finite duration impulse response (FIR) digital filter to approximate a desired spectral response is treated in this paper. The philosophy adopted is that for a given FIR filter structure, the filter coefficients can be designed to provide a minimum mean-squared error (MMSE) estimate of a random signal sequence (the design-signal) imbedded in a random noise sequence. By treating the signal and noise covariance functions as design parameters, one can design FIR filters with spectral responses that approximate the power spectral density of the design-signal. For signal processing applications that require some attention to signal fidelity, as well as noise rejection, the MMSE philosophy seems appropriate (as opposed to a maximum signal-to-noise ratio philosophy, for example).

Several practical designs are presented that emphasize the simplicity of the design technique and illustrate the selection of design parameters. The designs show quite dramatically that the MMSE design technique can be competitive with existing low-pass and bandpass design techniques.

Finally, considerable attention is given to an efficient Toeplitz matrix inversion algorithm that permits rapid inversion of the covariance matrices that arise in the MMSE design. The resulting computation times for the design of high-order filters ( $N = 128$ , e.g.) appear to be shorter than computation times for competing algorithms.

## I. INTRODUCTION

THE PROBLEM of designing digital filters to approximate "ideal" spectral characteristics has received considerable attention in recent years (e.g., [1],[2]). Many different approaches have been used in the design of finite duration impulse response (FIR) filters [3]–[13]. The majority of these FIR filter design techniques employ either an iterative frequency sampling technique or a window technique as, for example, in [6] and [11], respectively. An alternative approach adopted in this paper is to treat the FIR filter as an estimator structure to provide a minimum mean-squared error (MMSE) estimate of some design-signal. The MMSE philosophy

has enjoyed great popularity in control and communication applications where signal fidelity is often an important consideration. More recently, the MMSE philosophy has found its way into the digital filtering literature [8]. The present paper is related in philosophy to [8], but extends the MMSE methodology to the design of linear phase MMSE low-pass and bandpass FIR filters with computation design times and spectral characteristics which appear to be competitive with existing design techniques. The large number of examples in [6] has prompted the choice of examples in this paper to coincide with those of [6] for comparison purposes. The choices of design parameters in this paper which lead to low-pass and bandpass designs incorporate the idea of a "don't care" region or a transition band which is related to the incompletely specified least mean square error method presented in [10].

### *Methodology*

The underlying theme of this paper is the use of an hypothetical design-signal that has a power spectral density equal to the desired spectral response of the FIR filter. The design-signal is assumed to be a stationary random sequence imbedded in an additive stationary noise sequence and/or a strong adjacent-band interference sequence. The goal of the filter design, then, is to choose the filter weighting coefficients so that the filter output will be an MMSE estimate of the design-signal. By treating the noise and interference spectra as design parameters one can achieve a family of FIR filter designs and then choose the design that best satisfies the requirements of a particular application.

It should be emphasized that specifications such as in-band and out-of-band ripple, detailed transition-band behavior, and other more classical digital filter specifications do not (and, indeed, need not) arise in our procedures. However, by judiciously choosing signal, noise, and interference spectra, the designer can exercise implicit control over such specifications and obtain filters with excellent passband ripple and side-lobe characteristics.

Manuscript received March 23, 1973; revised January 3, 1974. This work was supported in part by the Naval Undersea Center, San Diego, Calif. under Grant N00123-73-C-1375 and the Office of Naval Research under Grant N00014-67-A-0299-0019.

The authors are with the Department of Electrical Engineering, Colorado State University, Fort Collins, Colo. 80521.

Results

Several MMSE designs are presented for low-pass and bandpass FIR digital filters. One comb filter is designed to illustrate the versatility of the method. Each design assumes a perfectly bandlimited signal with known center frequency and bandwidth. Similar specifications are often employed in more conventional designs.

The results presented in this paper indicate that clever choices of signal, noise, and interference spectra can lead to designs that are competitive with other published designs. A particularly attractive feature of the results is the modest computational times required to realize the filters of interest. Each design requires a simple matrix inversion that is effected very efficiently with a recently published Toeplitz matrix inversion algorithm [14].

II. THE FILTER MODEL

An FIR tapped delay line filter structure is illustrated in Fig. 1. The structure consists of a tapped delay line with  $N$  taps,  $N - 1$  ideal time delays ( $D$ ), and  $N$  weights  $\{w_i, i = 1, 2, \dots, N\}$ . The input to the filter is assumed to be a stationary random sequence,  $\{x(kT), k = 0, \pm 1, \pm 2, \dots\}$ , with sampling interval  $T$ . Note that  $D$  must be an integer multiple of  $T$ . It will be convenient to denote the  $N$  filter weighting coefficients by the  $(N \times 1)$  vector,

$$W = (w_1, w_2, \dots, w_N)', \quad (1)$$

where ' denotes transpose.

The data at the  $N$  taps of the tapped delay line at time  $kT$  can be represented by the  $(N \times 1)$  vector,

$$X(kT) = S(kT) + N(kT) \quad (2)$$

where  $S(kT)$  and  $N(kT)$  are, respectively, signal and noise components of the data vector:

$$\begin{aligned} S'(kT) &= [s_1(kT), s_2(kT), \dots, s_N(kT)] \\ N'(kT) &= [n_1(kT), n_2(kT), \dots, n_N(kT)]. \end{aligned} \quad (3)$$

Signal and Noise Covariance Functions

For convenience, the signal and noise sequences  $\{s_i(kT), k = 0, \pm 1, \pm 2, \dots\}$  and  $\{n_i(kT), k = 0, \pm 1, \pm 2, \dots\}$  are assumed to be samples of uncorrelated, zero-mean, wide-sense stationary continuous time random processes,  $s(t)$ , and  $n(t)$ , respectively. Define the signal and noise covariance functions,  $R_s(\tau)$  and  $R_n(\tau)$  by

$$\begin{aligned} R_s(\tau) &= E\{s(t)s(t + \tau)\}, \\ R_n(\tau) &= E\{n(t)n(t + \tau)\}, \end{aligned} \quad (4)$$

where  $E\{\cdot\}$  denotes statistical expectation.

Define the data covariance matrix  $R_{XX}$  by

$$\begin{aligned} R_{XX} &= E\{X(kT)X'(kT)\} \\ &= R_{SS} + R_{NN}, \end{aligned} \quad (5)$$

where the signal and noise covariance matrices are, respectively,

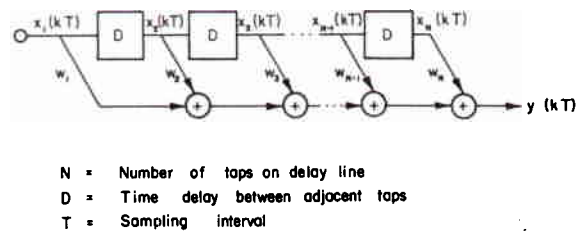


Fig. 1. Filter model.

- N = Number of taps on delay line
- D = Time delay between adjacent taps
- T = Sampling interval

$$\begin{aligned} R_{SS} &= E\{S(kT)S'(kT)\} \\ R_{NN} &= E\{N(kT)N'(kT)\}. \end{aligned} \quad (6)$$

It is noted that  $trR_{SS} = N\sigma_s^2$  and  $trR_{NN} = N\sigma_n^2$ , where  $\sigma_s^2$  is the signal variance per tap and  $\sigma_n^2$  is the noise variance per tap. The  $ij$ th elements of  $R_{SS}$  and  $R_{NN}$  are given by  $R_s[(i - j)D]$  and  $R_n[(i - j)D]$ , respectively.

One other statistical parameter of interest is the so-called signal covariance vector

$$P_{s1} = E\{s_1(kT)S(kT)\}. \quad (7)$$

Noting that the  $i$ th element of  $P_{s1}$  is given by  $R_s[(i - l)D]$ , the interpretation of  $s_1(kT)$  can be generalized to include noninteger  $l$ , corresponding to  $s_1(kT - (l - 1)D)$ .

Filter Frequency Response

The magnitude-squared frequency response,  $|H(f)|^2$ , of the FIR filter is defined to be

$$|H(f)|^2 = \left| \sum_{k=1}^N w_k \exp\{-j2\pi f(k - 1)D\} \right|^2. \quad (8)$$

It is worth emphasizing that for  $f = l/ND, l = 0, 1, \dots, N - 1$ ,  $H(f)$  is the discrete Fourier transform (DFT) of  $W$ . A computationally efficient method of computing (8) for a large number of equally spaced frequency points is to augment  $W$  with zeros, i.e., replace  $W'$  by  $(w_1, w_2, \dots, w_N, 0, 0, \dots, 0)$  and use the fast Fourier transform (FFT).

III. THE MMSE FILTER DESIGN TECHNIQUE

The MMSE problem is one of designing the weight vector  $W$  so that the filter output  $y(kT)$  (see Fig. 1) is the MMSE estimate of the design-signal sequence  $\{s_i(kT), k = 0, \pm 1, \pm 2, \dots\}$ . Recall that  $s_i(kT)$  is the design-signal observed at time  $kT - (l - 1)D$  at the input of the tapped delay line.

The output of the filter,  $y(kT)$ , is given by

$$y(kT) = W'X(kT). \quad (9)$$

Therefore, the mean-squared error in estimating  $s_i(kT)$  with  $y(kT)$  is

$$\begin{aligned} \xi(W) &= E\{[y(kT) - s_i(kT)]^2\} \\ &= W'R_{XX}W - 2W'P_{s1} + \sigma_s^2, \end{aligned} \quad (10)$$

where  $\sigma_s^2 = R_s(0)$ . Taking the gradient of  $\xi(W)$  with respect to  $W$ , one can easily show that the well known

Wiener solution for the minimizing weight vector is

$$W_{MMSE} = R_{XX}^{-1}P_{s,i} \quad (11)$$

### Computational Considerations

The design of an MMSE filter requires inversion of the  $(N \times N)$  covariance matrix  $R_{XX}$ . Recently, a computationally efficient algorithm [14] has been developed for the inversion of such matrices. The inversion algorithm exploits the Toeplitz nature of  $R_{XX}$ , i.e., the algorithm makes efficient use of the fact that  $r_{ij}$ , the  $ij$ th element of  $R_{XX}$  depends only on  $|i - j|$ :

$$\begin{aligned} r_{ij} &= E\{x_i(kT)x_j(kT)\} \\ &= E\{x_i(kT)x_i[kT + (j - i)D]\} \\ &= R_x(|i - j|D) \end{aligned} \quad (12)$$

where  $R_x(\cdot)$  is the data covariance function, i.e.,  $R_x(\cdot) = R_s(\cdot) + R_n(\cdot)$ . A Fortran subroutine making use of the algorithm is presented in the Appendix. The routine is capable of computing the solution of (11) for  $N = 256$  in less than four s of central processor time on a CDC 6400 computer.

### A Sufficient Condition for Linear Phase

A well known result for FIR filters is that a sufficient condition for linear phase is that the weight vector be symmetric about its center, i.e.,

$$w_i = w_{N-i+1} \quad (13)$$

for all  $i \in \{1, 2, \dots, N\}$ . It has been shown [15] that the inverse of a persymmetric (symmetric about both main diagonals) matrix is also persymmetric. Since  $R_{XX}$  is persymmetric it follows easily that if the elements of  $P_{s,i}$  satisfy (13), then a filter designed using (11) will have linear phase. For  $N$  even or odd, choosing the  $i$ th element of  $P_{s,i}$  to be  $R_s[(i - (N + 1)/2)D]$  will result in linear phase MMSE filters.

## IV. DESIGN CONSIDERATIONS

As the discussion of the previous sections has shown, there are several design parameters that must be rationally selected in the design of an MMSE filter. In this section we discuss these design parameters and show how one can choose  $R_s(\tau)$  and  $R_n(\tau)$  to achieve effective low-pass and bandpass designs.

### Signal Covariance Function, $R_s(\tau)$

The signal covariance function  $R_s(\tau)$  is uniquely determined as the inverse Fourier transform of the desired magnitude-squared frequency function of the FIR filter between  $-f_f$  and  $f_f$ , where  $f_f = 1/2D$  is the foldover frequency of the FIR filter. For example, consider the perfectly bandlimited spectrum  $S(f)$  illustrated with the solid lines of Fig. 2(a). The inverse Fourier transform of  $S(f)$ ,  $R_s(\tau)$ , is given by

$$R_s(\tau) = 2BW \frac{\sin(\pi BW\tau)}{\pi BW\tau} \cos 2\pi f_0\tau \quad (14)$$

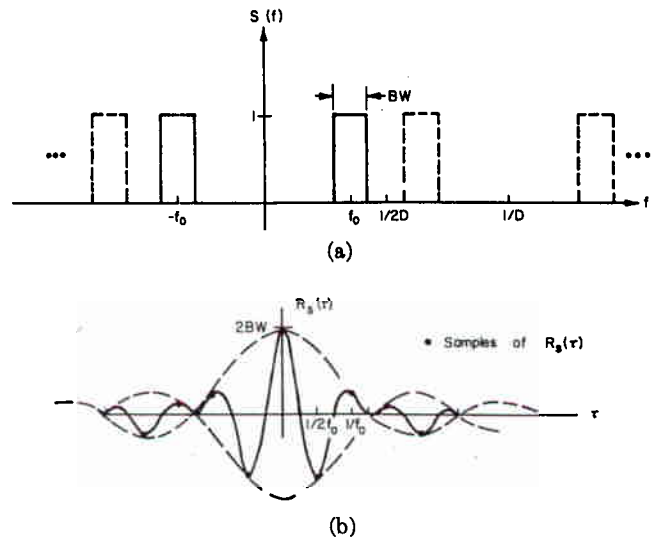


Fig. 2. Signal spectral model for bandpass designs. (a) Desired spectral response,  $S(f)$ . (b) Inverse transform of  $S(f)$ .

The function  $R_s(\tau)$  illustrated in Fig. 2(b) may be thought of as the covariance function of some zero-mean, wide-sense stationary design-signal  $s(t)$  with power spectral density  $S(f)$ . The spectral region where  $S(f)$  is nonzero will be referred to as the passband. It is obvious that such a selection of  $S(f)$  will lead to band-pass filter designs.

### Noise Covariance Function, $R_n(\tau)$

Once  $R_s(\tau)$  is fixed, the noise covariance function  $R_n(\tau)$  may be chosen to reflect the relative costs of passing a component of the noise and distorting the signal. For conventional low-pass and bandpass designs,  $R_n(\tau)$  will be the inverse Fourier transform of the power spectral density,  $S_n(f)$  of a broadband interference.  $S_n(f)$  will be nonzero in a spectral region which will be referred to as the stopband, as illustrated in Fig. 3. The spectral level of  $S_n(f)$  will determine the price paid for passing a signal in the stopband relative to the price paid for distorting a signal in the passband; thus the level of  $S_n(f)$  is a free design parameter. The spectral region between the passband and the stopband will be referred to as the transition band. These heuristic comments are formalized in the following paragraph.

From (11), the mean-squared error in estimating  $s_i(kT)$  when only the signal is present is given by

$$\begin{aligned} \xi_s(W_{MMSE}) &= E\{[W_{MMSE}'S(kT) - s_i(kT)]^2\} \\ &= W_{MMSE}'R_{SS}W_{MMSE} - 2W_{MMSE}'P_{s,i} + \sigma_s^2 \end{aligned} \quad (15)$$

From the definitions of  $R_{SS}$  and  $P_{s,i}$  it should be clear that one may interpret  $\xi_s(W_{MMSE})$  as "passband distortion." Making use of the well known fact that the mean-squared error,  $\xi(W_{MMSE})$  is always less than or equal to the signal variance,  $\sigma_s^2$ , we have

$$0 \leq \xi_s(W_{MMSE}) + W_{MMSE}'R_{NN}W_{MMSE} \leq \sigma_s^2 \quad (16)$$

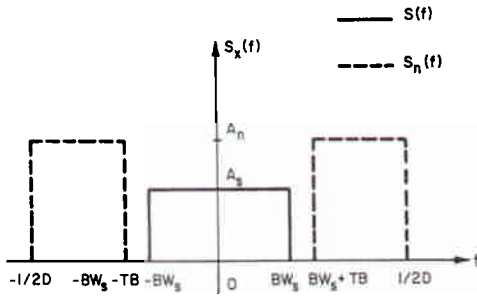


Fig. 3. Spectral model for low-pass filter designs.

where  $W_{MMSE}'R_{NN}W_{MMSE}$  is the error variance due to the stopband noise (or broadband interference). If  $R_{NN} = A_n \rho_{NN}$  is the noise covariance matrix for a broadband interference of spectral height  $A_n$ , (16) becomes

$$0 \leq W_{MMSE}'\rho_{NN}W_{MMSE} \leq \frac{1}{A_n} [\sigma_s^2 - \xi_s(W_{MMSE})] \leq \frac{\sigma_s^2}{A_n} \quad (17)$$

and it follows that increasing  $A_n$  will decrease  $W_{MMSE}'\rho_{NN}W_{MMSE}$ , which is directly related to the stopband sidelobe level, at the expense of increasing  $\xi_s(W_{MMSE})$ , the passband distortion.

*Estimation Point, l*

Filter applications for which a delayed estimate of the signal component at the input of the FIR filter is acceptable permit a choice of delay  $(l - 1)D$  that can further reduce the mean-square estimation error and, hence, yield a more desirable spectral response than other choices of delay. From (11) it is easily established that the minimum mean-square error,  $\xi(W_{MMSE})$ , in estimating  $s_l(kT)$  is given by

$$\begin{aligned} \xi(W_{MMSE}) &= \sigma_s^2 - W_{MMSE}'P_{s,l} \\ &= \sigma_s^2 - P_{s,l}'R_{XX}^{-1}P_{s,l}. \end{aligned} \quad (18)$$

The choice of  $l$  that minimizes  $\xi(W_{MMSE})$  is that value of  $l$  for which the quadratic form  $P_{s,l}'R_{XX}^{-1}P_{s,l}$  is maximized. Rather than maximize  $P_{s,l}'R_{XX}^{-1}P_{s,l}$ , a procedure that depends on  $R_{XX}^{-1}$ , consider maximizing the following bound:

$$\begin{aligned} P_{s,l}'R_{XX}^{-1}P_{s,l} &= \text{tr} \{R_{XX}^{-1}P_{s,l}P_{s,l}'\} \\ &\leq \text{tr} \{R_{XX}^{-1}\} \text{tr} \{P_{s,l}P_{s,l}'\} \\ &= \text{tr} \{R_{XX}^{-1}\} P_{s,l}'P_{s,l}. \end{aligned} \quad (19)$$

From (19), a logical choice for the delay  $(l - 1)D$  is one that maximizes the norm of  $P_{s,l}$ . Choosing  $l$  as near as possible to the center of the tapped delay line results in an excellent approximation to the maximum achievable  $\|P_{s,l}\|^2$ . This choice coincides nicely with the discussion in Section III which suggested that for  $l = (N + 1)/2$ , linear phase filters would result.

*Normalization Procedures*

The level of the MMSE filter spectral response (equivalently, the norm of the weight vector) depends on the

signal and noise covariance matrices. Consequently, the weight vector designed by the MMSE method must be scaled in order to achieve the desired spectral level. One approach to scaling would be to select a frequency,  $f_d$ , where a spectral level,  $A$ , is required, and then compute a scaled weight vector

$$W_s = W \left( \frac{A}{S(f_d)} \right)^{1/2} \quad (20)$$

where  $S(f_d)$  is the spectral response of  $W$  at  $f = f_d$  [ $S(f_d) = |H(f_d)|^2$  from (8)].

An alternative approach is to require that the output variance of the filter be  $\sigma_v^2$  when driven by a discrete white noise process  $n(kT)$  of unit spectral height. It follows easily that the noise covariance matrix  $R_{NN}$  of (6) is given by  $R_{NN} = (2/D)I$ . Thus the filter output variance is given by

$$\begin{aligned} \sigma_v^2 &= W'R_{NN}W \\ &= \frac{2}{D} W'W. \end{aligned} \quad (21)$$

Now consider use of the following scaled weight vector:

$$W_s = W \left( \frac{D\sigma_v^2}{2W'W} \right)^{1/2}. \quad (22)$$

It follows from (22) that the resulting filter output variance is  $\sigma_v^2 = \sigma_s^2$ .

V. DESIGN PERFORMANCE

In this section we discuss the performance of the MMSE-designed low-pass filter for several choices of design parameters. The spectral model of Fig. 3 is used throughout this section. A flow chart for the MMSE design technique is shown in Fig. 4. More conventional design techniques begin the design with specification of filter bandwidth, transition band, and allowable passband ripple and sidelobe height; the present technique calls for specification of the intended signal and noise environment in which the filter is to be used. By treating the noise environment as a design parameter, one can obtain a family of filter designs and observe passband ripple and maximum sidelobe level for comparison with more conventional designs.

*Performance Measures*

A typical magnitude-squared frequency response  $|H(f)|^2$  is shown as the solid line in Fig. 5. The design-signal power spectral density,  $S(f)$ , is shown as the dotted line. We define the passband ripple,  $R_1$ , as

$$R_1 = 10 \log_{10} \left\{ \text{maximum}_{f_1, f_2 \in [0, BW_s]} \frac{|H(f_1)|^2}{|H(f_2)|^2} \right\}. \quad (23)$$

The maximum sidelobe height,  $S_1$ , is defined by

$$S_1 = 10 \log_{10} \left\{ \text{maximum}_{f \in [BW_s + TB, f_f]} |H(f)|^2 \right\}. \quad (24)$$

Another performance measure of interest is the maximum

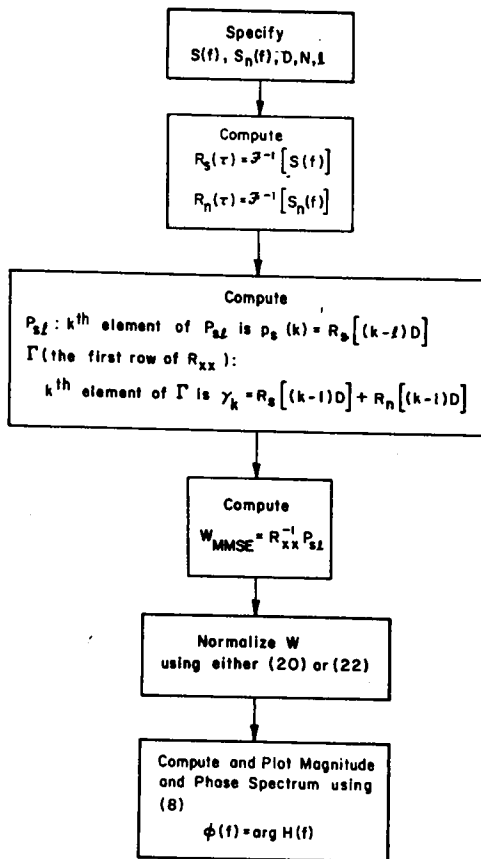


Fig. 4. Flow chart for the MMSE design technique.

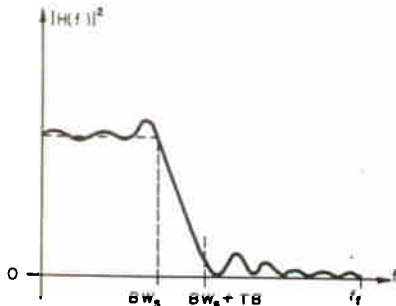


Fig. 5. Typical magnitude-squared transfer function for FIR filter.

of  $|H(f)|^2$  for frequencies greater than the first frequency,  $f_s$ , greater than  $BW_s$ , at which the slope of  $|H(f)|^2$  changes from negative to positive. Define  $S_2$  by

$$S_2 = 10 \log_{10} \left\{ \text{maximum}_{f \in [f_s, f_s]} |H(f)|^2 \right\}. \quad (25)$$

The performance measures  $S_2$  and  $f_s$  are of interest because the *effective* transition band (defined as  $f_s - BW_s$ ) cannot be specified *a priori*.<sup>1</sup> However, in all cases tried the difference between  $f_s - BW_s$  and  $TB$  was less than  $1/2N$ . We reiterate that this discrepancy between  $TB$  and  $f_s - BW_s$  in no way detracts from the optimality of

<sup>1</sup> Actually the discrepancy between effective transition band and design transition band is not unique to this design. That is, other design procedures often lead to slight differences between  $TB$  and  $f_s - BW_s$ ; in fact, there appears to be no universal agreement concerning the proper definition of effective transition band.

the filter, i.e., the filter provides an MMSE estimate of the low-pass process characterized by the signal spectrum of Fig. 3 when the process is immersed in bandpass, adjacent channel interference.

#### Effects of Parameters on the Performance Measures

A large number of low-pass filters have been designed to illustrate the effects of the design parameters on the passband ripple and sidelobe level. Specifically, filters have been designed for  $BW_s \in \{0.1, 0.2, 0.3, 0.4, 0.5\}$ ,  $f_s = 1.0$ ,  $A_n = 1.0$ ,  $A_n \in \{10^2, 10^4, 10^6\}$ ,  $N \in \{32, 64, 128, 256\}$  and  $TB \in \{2/N, 4/N, 6/N, 8/N, 10/N\}$ . Note that a different set of transition bands has been used for each value of  $N$ . The results indicate no dramatic difference in maximum sidelobe height or passband ripple for the values of bandwidth used.<sup>2</sup> Fig. 6 shows the effects of the parameters  $A_n$ , the interference level, and  $TB$ , the transition band, on the passband ripple,  $R_1$ , for  $N \in \{32, 64, 128, 256\}$ , and  $BW_s \in \{0.1, 0.2, 0.3, 0.4, 0.5\}$ . Fig. 7 shows the effects of the parameters  $A_n$  and  $TB$  on the maximum sidelobe level,  $S_1$ . Similarly, Fig. 8 shows the effects of the parameters  $A_n$  and  $TB$  on the performance measure  $S_2$ . Also shown in Figs. 7 and 8 is the range of  $S_1$  from the data given in [6] for  $BW_s \in \{0.1, 0.5\}$ ,  $TB \in \{4/N, 6/N, 8/N\}$ , and  $N \in \{32, 64, 128, 256\}$ . Figs. 7 and 8 illustrate the competitive nature of the MMSE filter when rated according to conventional filter performance measures.

#### Example Designs

In order to illustrate the performance of the MMSE design technique, several practical designs are shown in Figs. 9–11.

Figs. 9(a) and 9(b) show  $|H(f)|^2$  for a low-pass filter designed with  $BW_s = 0.2$ ,  $TB = 1/16$ , and  $A_n = 10^3$  for  $N = 32$  and 128 respectively; these designs illustrate the effect of increasing  $N$  without changing any other parameter. Fig. 9(c) shows a low-pass filter designed with  $BW_s = 0.2$ ,  $TB = 1/32$ , and  $A_n = 10^3$  for  $N = 256$ . Comparing Figs. 9(b) and 9(c), we note that decreasing  $TB$  by a factor of 2 and increasing  $N$  by a factor of 2 does not markedly change any performance measure, except the effective transition band, as one would expect from Figs. 6–8.

Fig. 10(a) shows the appropriate spectral model for bandpass designs. Figs. 10(b) and 10(c) show  $|H(f)|^2$  for  $f_0 = 61/128$ ,  $TB = 1/16$ ,  $BW_s = 15/128$ ,  $N = 128$ , and  $A_n = 10^6$  and  $10^9$  respectively. The above parameters were chosen to coincide with the designs given as Figs. 26–28 in [6]. Note the decrease in maximum sidelobe height and the increase in passband ripple with an increase in  $A_n$ .

A constant- $Q$  comb filter was designed using the spectral

<sup>2</sup> The single exception to this is the case where  $BW_s = 0.1$ ,  $N = 32$ ,  $TB = 1/16$ , for which an increase in  $A_n$  beyond  $10^3$  makes no significant difference. For this reason this case is not included in any of the figures.

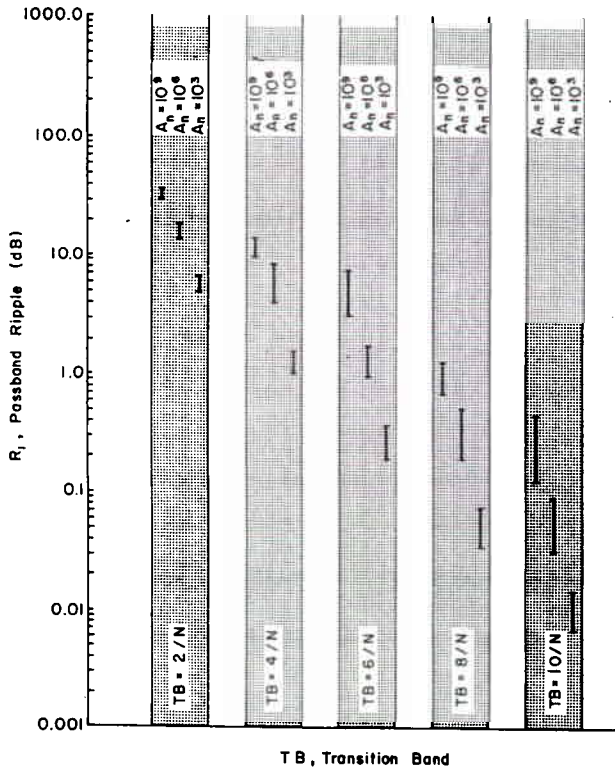


Fig 6. Passband ripple,  $R_1$ , as a function of transition band.

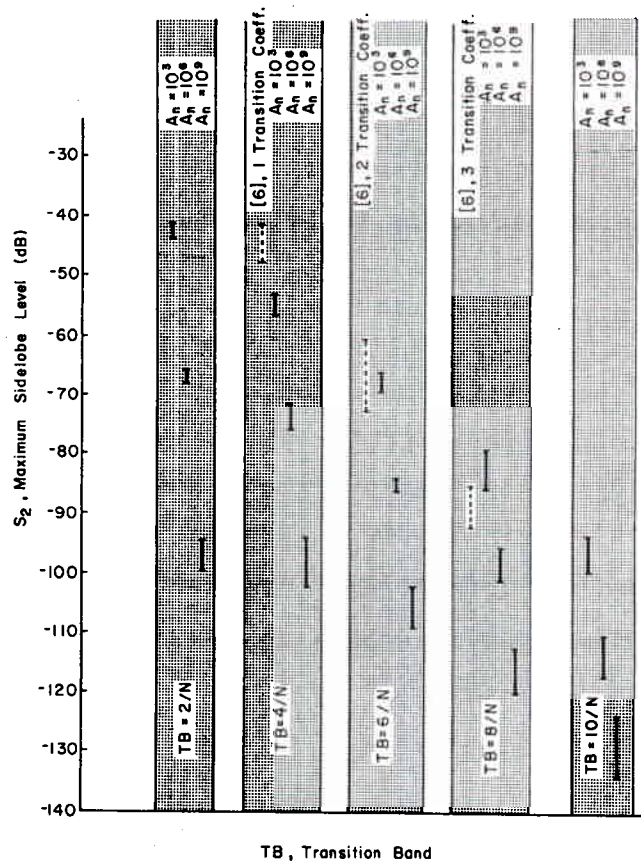


Fig 8. Maximum sidelobe height,  $S_2$ , as a function of transition band.

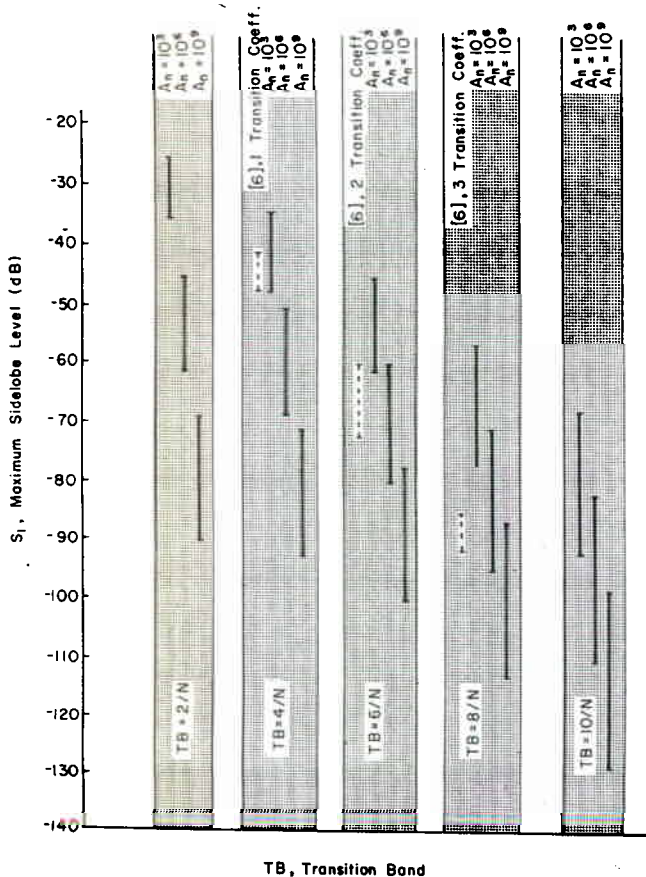


Fig 7. Maximum sidelobe height,  $S_1$ , as a function of transition band.

model of Fig. 11(a) with  $A_n = 10^3$ ; the magnitude-squared frequency response of the MMSE filter is shown in Fig. 11(b). This example shows the versatility of the MMSE design technique for piecewise-constant spectral models. There is, however, no inherent reason why the design technique cannot be extended to include more general spectral models.

VII. CONCLUSIONS

The design philosophy presented in this paper encourages the designer to treat the FIR filter as an estimator structure and to specify the free design parameters in a way directly related to the intended application of the filter. Some connections between these parameters and classical filter performance measures have been advanced.

Several designs have been presented for hypothetical signal-interference-noise applications where the motivation is to obtain effective MMSE estimates of low-pass and bandpass signals immersed in adjacent channel interference. By treating the interference level and bandwidth as design parameters, the authors have obtained low-pass and bandpass, and comb filter designs with passband and stopband properties that are competitive with existing designs [6]. These properties are summarized in Figs. 6-11.

The computation times required to design the class of MMSE filters discussed in this paper appear to be markedly shorter than the times required for other FIR

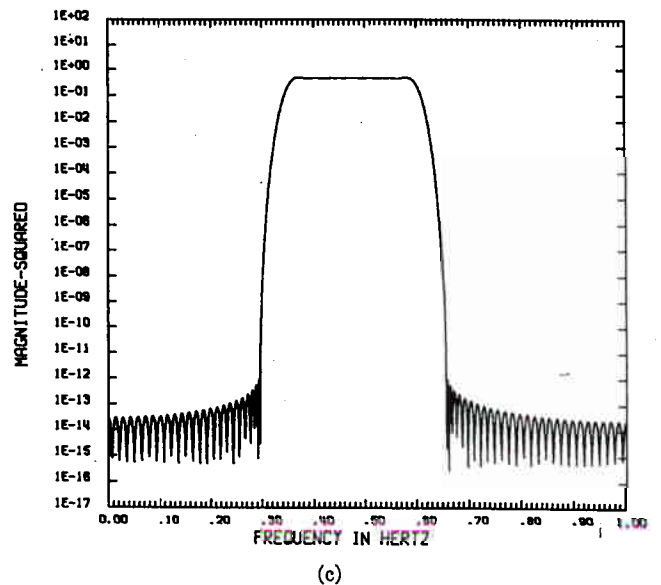
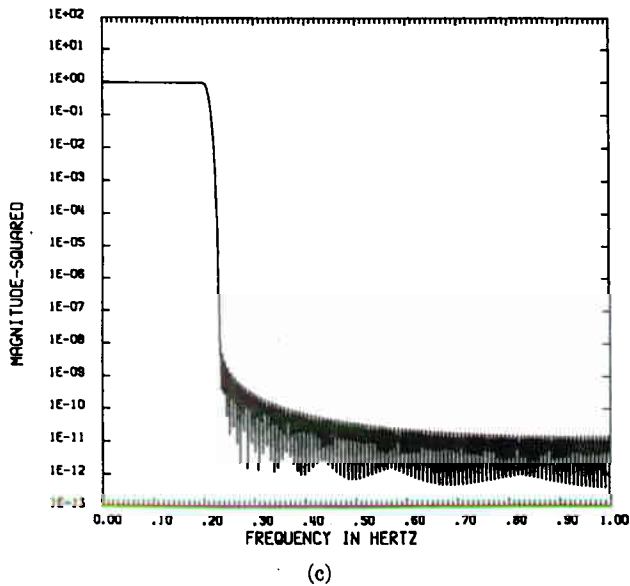
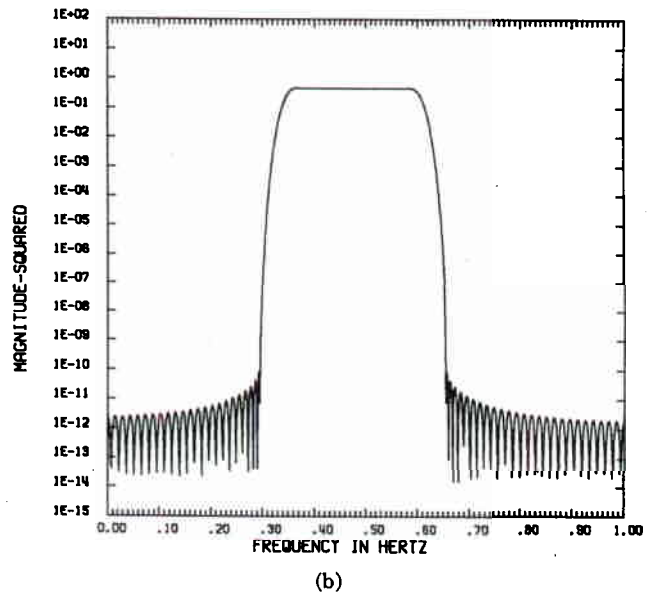
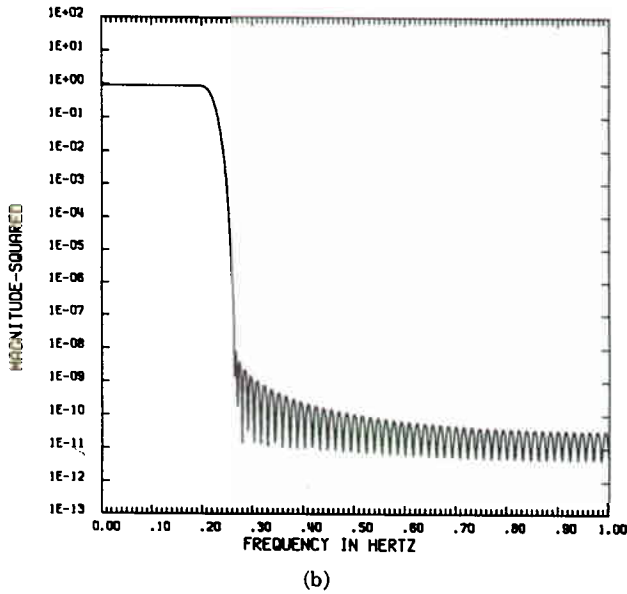
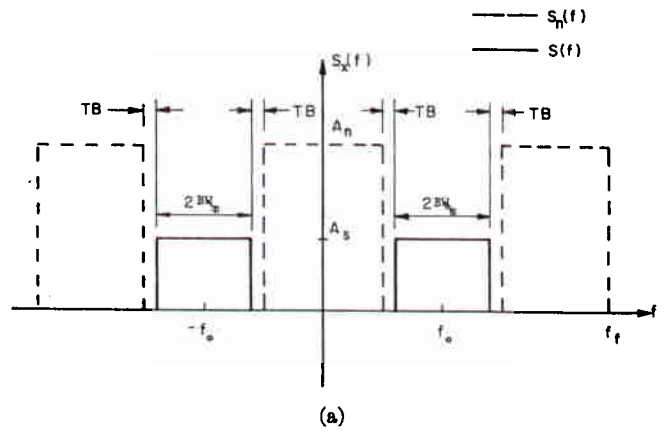
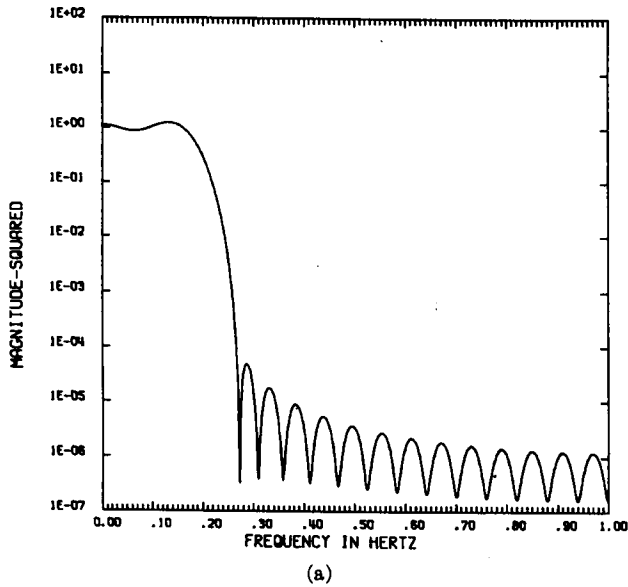


Fig. 9. Low-pass example designs: (a)  $BW_n = 0.2$ ,  $TB = 1/16$ ,  $A_n = 10^4$ ,  $N = 32$ . (b)  $BW_n = 0.2$ ,  $TB = 1/16$ ,  $A_n = 10^4$ ,  $N = 128$ . (c)  $BW_n = 0.2$ ,  $TB = 1/32$ ,  $A_n = 10^4$ ,  $N = 256$ .

Fig. 10. (a) Spectral model for bandpass filter designs. (b) Bandpass example design:  $f_0 = 61/128$ ,  $TB = 1/16$ ,  $BW_n = 15/128$ ,  $N = 128$ ,  $A_n = 10^4$ . (c) Bandpass example design:  $f_0 = 61/128$ ,  $TB = 1/16$ ,  $BW_n = 15/128$ ,  $N = 128$ ,  $A_n = 10^9$ .





- Trans. Audio Electroacoust.*, vol. AU-18, pp. 464-470, Dec. 1970.
- [8] W. C. Kellogg, "Time domain design of nonrecursive least mean-square digital filters," *IEEE Trans. Audio Electroacoust.*, vol. AU-20, pp. 155-158, June 1972.
- [9] A. Papoulis and M. S. Bertran, "Digital filtering and prolate functions," *IEEE Trans. Circuit Theory*, vol. CT-19, pp. 674-681, Nov. 1972.
- [10] D. W. Tufts and J. T. Francis, "Designing digital low-pass filters—comparison of some methods and criteria," *IEEE Trans. Audio Electroacoust.*, vol. AU-18, pp. 487-494, Dec. 1970.
- [11] J. F. Kaiser, "Digital filters," in *System Analysis by Digital Computers*, F. F. Kuo and J. F. Kaiser, Eds. New York: Wiley, 1966, ch. 7.
- [12] T. W. Parks and J. H. McClellan, "Chebyshev approximation for nonrecursive digital filters with linear phase," *IEEE Trans. Circuit Theory*, vol. CT-19, pp. 189-194, Mar. 1972.
- [13] H. S. Hersey *et al.*, "Interactive minimax design of linear-phase nonrecursive digital filters subject to upper and lower function constraints," *IEEE Trans. Audio Electroacoust.* (Corresp.), vol. AU-20, pp. 171-173, June 1972.
- [14] D. H. Preis, "The Toeplitz matrix: its occurrence in antenna problems and a rapid inversion algorithm," *IEEE Trans. Antennas Propagat.* (Commun.), vol. AP-20, pp. 204-206, Mar. 1972.
- [15] S. Zohar, "Toeplitz matrix inversion: the algorithm of W. F. Trench," *J. Ass. Comput. Mach.*, vol. 16, pp. 592-601, Oct. 1969.